

Accepted Manuscript

Design, Synthesis, and Structure-Activity Relationships of Pyrimido[4,5-*b*]indole-4-amines as Microtubule Depolymerizing Agents that are Effective against Multidrug Resistant Cells

Ravi Kumar Vyas Devambatla, Wei Li, Nilesh Zaware, Shruti Choudhary, Ernest Hamel, Susan L. Mooberry, Aleem Gangjee

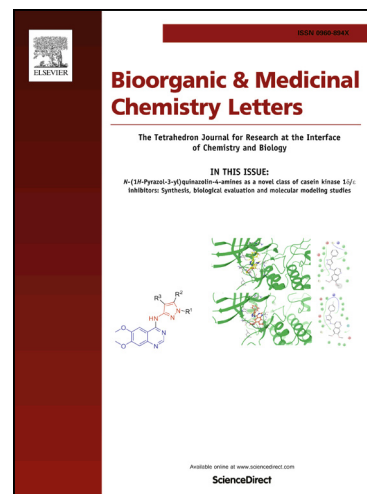
PII: S0960-894X(17)30583-8
DOI: <http://dx.doi.org/10.1016/j.bmcl.2017.05.085>
Reference: BMCL 25030

To appear in: *Bioorganic & Medicinal Chemistry Letters*

Received Date: 12 April 2017
Revised Date: 24 May 2017
Accepted Date: 27 May 2017

Please cite this article as: Devambatla, R.K.V., Li, W., Zaware, N., Choudhary, S., Hamel, E., Mooberry, S.L., Gangjee, A., Design, Synthesis, and Structure-Activity Relationships of Pyrimido[4,5-*b*]indole-4-amines as Microtubule Depolymerizing Agents that are Effective against Multidrug Resistant Cells, *Bioorganic & Medicinal Chemistry Letters* (2017), doi: <http://dx.doi.org/10.1016/j.bmcl.2017.05.085>

This is a PDF file of an unedited manuscript that has been accepted for publication. As a service to our customers we are providing this early version of the manuscript. The manuscript will undergo copyediting, typesetting, and review of the resulting proof before it is published in its final form. Please note that during the production process errors may be discovered which could affect the content, and all legal disclaimers that apply to the journal pertain.



Design, Synthesis, and Structure–Activity Relationships of Pyrimido[4,5-*b*]indole-4-amines as Microtubule Depolymerizing Agents that are Effective against Multidrug Resistant Cells

Ravi Kumar Vyas Devambatla^a, Wei Li^a, Nilesh Zaware^a, Shruti Choudhary^a, Ernest Hamel^b, Susan L. Mooberry^{c,†,*}, Aleem Gangjee^{a,†,*}

^a *Division of Medicinal Chemistry, Graduate School of Pharmaceutical Sciences, Duquesne University, 600 Forbes Avenue, Pittsburgh, PA 15282.*

^b *Screening Technologies Branch, Developmental Therapeutics Program, Division of Cancer Treatment and Diagnosis, Frederick National Laboratory for Cancer Research, National Institutes of Health, Frederick, MD 21702.*

^c *Department of Pharmacology, Cancer Therapy & Research Center, University of Texas Health Science Center at San Antonio, 7703 Floyd Curl Drive, San Antonio, TX 78229.*

† These authors contributed equally to this work.

* To whom correspondence should be addressed. For A.G.: phone, 412-396-6070; fax, 412-396-5593; e-mail, gangjee@duq.edu. For S.L.M.: phone, 210-567-4788; fax, 210-567-4300; e-mail, mooberry@uthscsa.edu.

Keywords: Microtubules; pyrimido[4,5-*b*]indoles; microtubule depolymerizing agents; multidrug resistance; conformational restriction

Abbreviations: National Cancer Institute (NCI); microtubule targeting agents (MTAs); combretastatin A-4 (CA-4); dimethyl sulfoxide (DMSO); Protein Data Bank (PDB); P-glycoprotein (Pgp); relative resistance (Rr); nuclear magnetic resonance (NMR).

Abstract

To identify the structural features of 9*H*-pyrimido[4,5-*b*]indoles as microtubule depolymerizers, pyrimido[4,5-*b*]indoles **2–8** with varied substituents at the 2-, 4- and 5-positions were designed and synthesized. Nucleophilic displacement of 2,5-substituted-4-chloro-pyrimido[4,5-*b*]indoles with appropriate arylamines was the final step employed in the synthesis of target compounds **2–8**. Compounds **2** and **6** had two-digit nanomolar potency (IC₅₀) against MDA-MB-435, SK-OV-3 and HeLa cancer cells in vitro. Compounds **2** and **6** also depolymerized microtubules comparable to the lead compound **1**. Compounds **2**, **3**, **6** and **8** were effective in cells expressing P-glycoprotein or the βIII isotype of tubulin, mechanisms that are associated with clinical drug resistance to microtubule targeting drugs. Proton NMR and molecular modeling studies were employed to identify the structural basis for the microtubule depolymerizing activity of pyrimido[4,5-*b*]indoles.

Microtubules are key components of the cytoskeleton for all eukaryotes and are involved in critical cellular processes including cell division, trafficking, signaling and migration.^{1, 2} These functions depend on the dynamic nature of microtubules, which arises from complex growth and shortening events related to GTP hydrolysis that is facilitated by microtubule associated proteins.³ Microtubule targeting agents (MTAs) disrupt microtubule dynamics by altering αβ tubulin heterodimer addition and loss, which in turn disrupts microtubule-dependent events. In vitro, microtubule disruption initiates mitotic arrest and cell death, but evidence suggests that additional mechanisms are involved in the clinical activity of microtubule targeting drugs.^{2, 4} These drugs are some of the most successful anticancer agents used clinically.¹ In addition, MTAs are the only class of cytotoxic anticancer agents effective against p53-mutant cell lines,

which constitute 39 of the 58 cell lines in the National Cancer Institute (NCI) 60-cancer cell line panel.^{5,6}

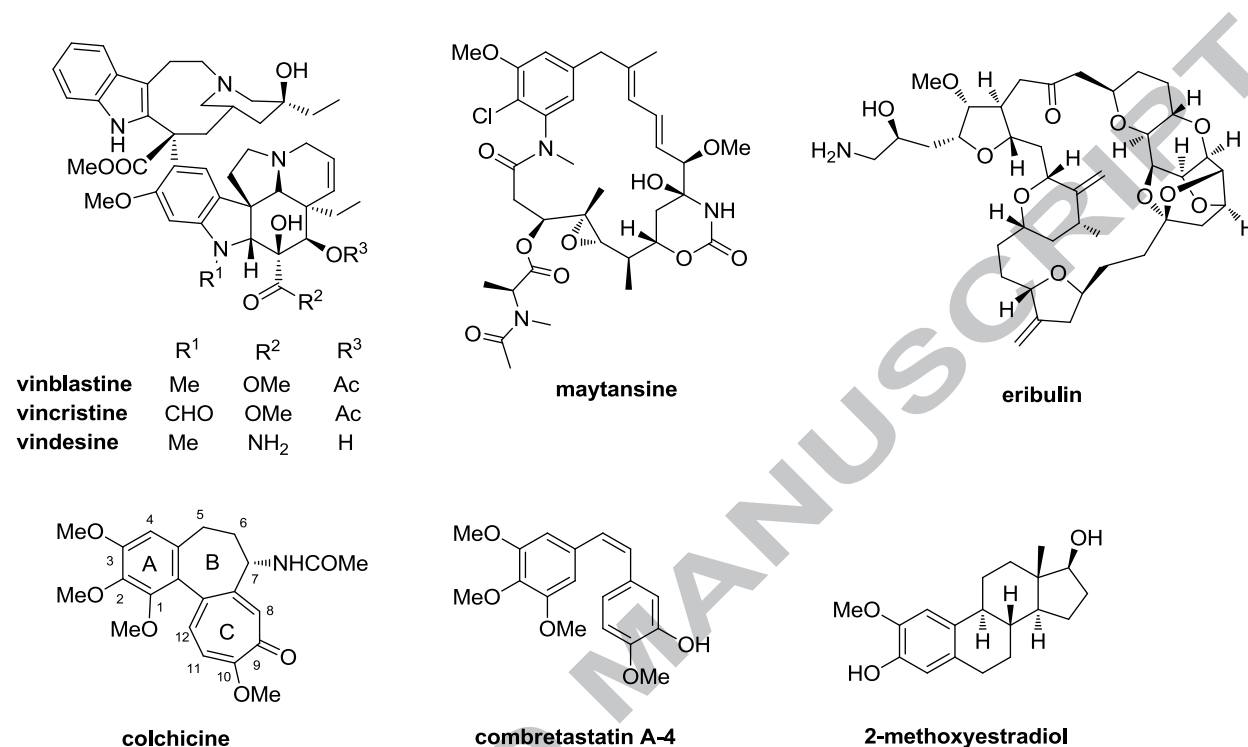


Figure 1. Structurally diverse microtubule depolymerizing agents.

MTAs are classified as microtubule polymerizing agents, which promote microtubule polymerization, or as microtubule depolymerizing agents, which inhibit microtubule polymerization. Microtubule depolymerizers can be further divided into three classes based on their tubulin binding site: the vinca domain, the maytansine site and the colchicine site. The vinca alkaloids, including vincristine, vinblastine and vindesine (Figure 1), bind competitively within the vinca site. The vinca alkaloids are indicated for both adult and pediatric cancers.⁷ Eribulin (Figure1), a simplified analog of halichondrin B,⁸ binds within the vinca domain, and has unique effects on microtubule dynamics.^{8,9} Structurally diverse natural products including rhizoxin and maytansine (Figure 1) bind to a different site on β -tubulin, referred to as the maytansine site.¹⁰ The occupancy of this site by maytansine causes microtubule

depolymerization by inhibiting longitudinal tubulin interactions.¹⁰ Eribulin and maytansine both have clinical utility, maytansine is the cytotoxin in the antibody-drug conjugate trastuzumab emtansine used for HER2-positive breast cancer¹¹ and eribulin is approved for the treatment of metastatic or locally advanced breast cancer¹² and liposarcoma.¹³ The colchicine site is a non-overlapping binding site located on β -tubulin at its interface with α -tubulin.^{14, 15} While colchicine (Figure 1) is too toxic for use in cancer therapy, multiple colchicine-site binding agents including combretastatin A-4 phosphate (CA-4P, fosbretabulin),¹⁶⁻¹⁹ combretastatin A-1 diphosphate (CA-1P, OXi4503),²⁰ and 2-methoxyestradiol^{21, 22} (Figure 1) were evaluated in early phase clinical trials. The microtubule polymerizers (stabilizers) that increase the density of microtubules in cells and disrupt microtubule dynamics include the taxanes, laulimalide, peloruside A, epothilones, zampanolide and taccalonolides.^{2, 23, 24} However, only paclitaxel, docetaxel and an epothilone B derivative ixabepilone are used clinically. Paclitaxel and docetaxel are widely used in the treatment of solid tumors such as breast, prostate, gastric, and lung cancers amongst others, ixabepilone is used in the US for the treatment of refractory metastatic breast cancer.²³

Multidrug resistance is a major factor in the failure of cancer chemotherapy.²⁵ Expression of the ABC transporter, P-glycoprotein (Pgp) or the expression of β III-tubulin are two major mechanisms of tumor resistance to taxanes and vinca alkaloids.^{26, 27} Development of MTAs that circumvent Pgp and/or β III-tubulin-mediated resistance²⁸ could have advantages in patients who fail to respond to current MTAs. Most of the colchicine site agents circumvent Pgp and β III-tubulin mediated resistance^{28, 29} and could be beneficial. However, thus far, no colchicine site agent has been approved as an anticancer agent. Hence, this site provides new opportunities for drug discovery.

Gangjee *et al.*²⁹ reported pyrimido[4,5-*b*]indole **1** (Figure 2) as a potent microtubule depolymerizer (EC₅₀ of 133 nM) with potent *in vitro* cytotoxic activity in MDA-MB-435 cells (IC₅₀ of 14.7 nM). Compound **1** is a colchicine site agent and it also circumvents clinically relevant Pgp and β III-tubulin mediated resistance. Compounds **2–8** (Figure 2) were designed to identify key structural features of **1** responsible for microtubule depolymerizing activities and binding within the colchicine site.

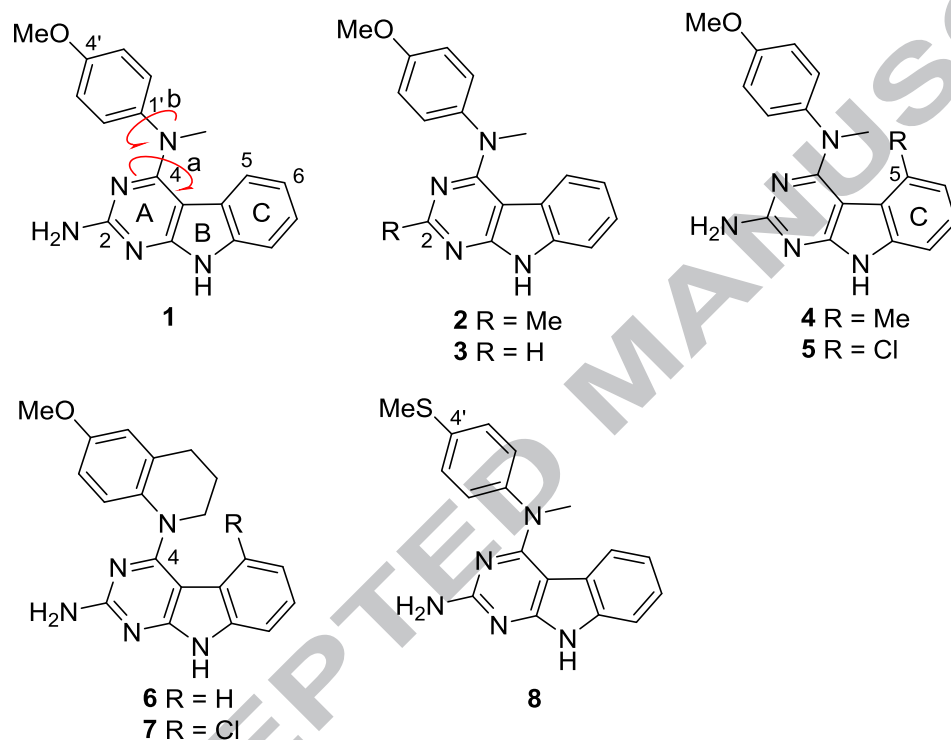
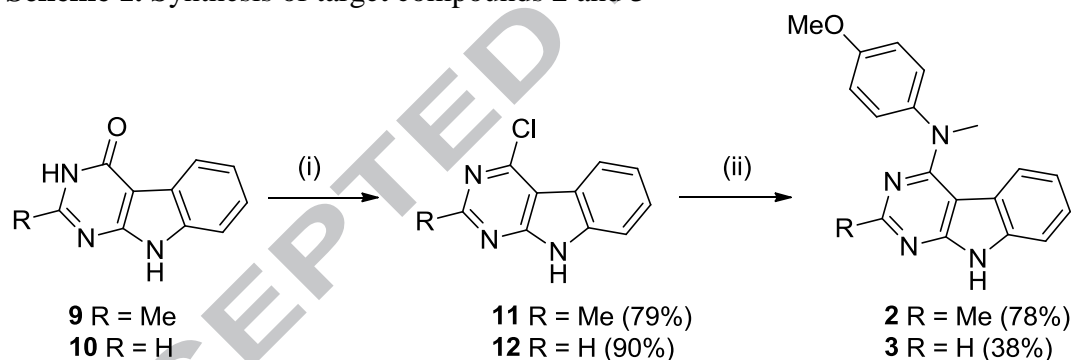


Figure 2. Parent pyrimido[4,5-*b*]indole **1** and target compounds **2–8**.

Compounds **2** and **3** (Figure 2) with 2-Me and 2-H substitutions, respectively, were designed to evaluate the importance of the 2-NH₂ group for microtubule depolymerizing activity. Similar substitutions were incorporated in the cyclopenta[*d*]pyrimidine series³⁰ and resulted in improved potency in some cases. Compounds **4** and **5**, which have different substitutions at the 5-position, were designed to evaluate the role of the electronics of the C-ring and/or hydrophobicity on microtubule depolymerization. Compounds **4** and **5**, in addition, conformationally restrict the

rotation around the N-C4 bond (a) in **1** (Figure 2) as well as the N-C1' bond (b) in **1** due to steric hindrance caused by the presence of a larger 5-Me or 5-Cl moiety respectively, instead of the 5-H in **1**. Compounds **6** and **7** were designed as conformationally restricted analogs by incorporating the bicyclic 6-methoxy-tetrahydroquinoline moiety onto the 4-position of the pyrimido[4,5-*b*]indole. Compared to the *N*-methylanilines, **1–5**, the tetrahydroquinoline moiety of **6** and **7** eliminates rotation around the b bond, thereby restricting the conformation of the phenyl ring. The restricted conformation of the phenyl group in **6** and **7** results in a much more rigid structure than **1** and **4**, respectively, but still maintains the phenyl and alkyl substitutions on the *N*⁴-position. Compound **8** was designed as a bioisostere of **1** by replacement of the 4'-OMe group with a 4'-SMe moiety to determine the bulk tolerance (O vs S) as well as the importance of hydrogen bonding.

Scheme 1. Synthesis of target compounds **2** and **3**^a

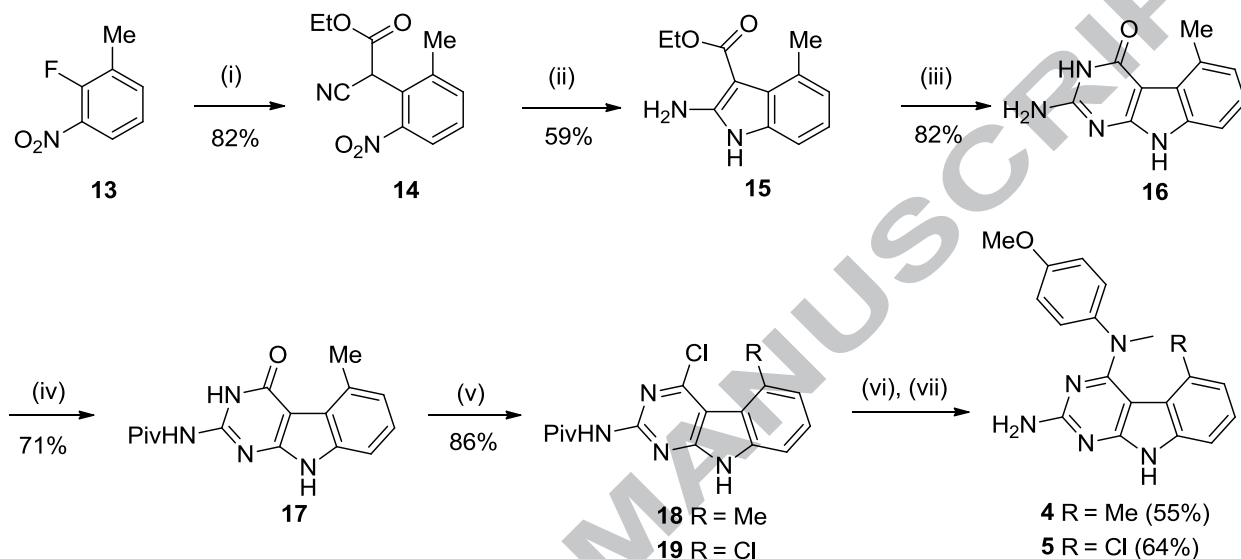


^aReagents and conditions: (i) POCl₃, reflux; (ii) 4-methoxy-*N*-methylaniline, conc. HCl (2 drops), BuOH, reflux.

Synthesis of target compounds **2** and **3** is shown in Scheme 1. Compounds **9**³¹ and **10**³² were synthesized using reported literature procedures. Treatment of **9** and **10** with POCl₃ afforded the 4-chloro-pyrimido[4,5-*b*]indoles **11** and **12**, respectively. Displacement of the 4-Cl of **11** and **12**

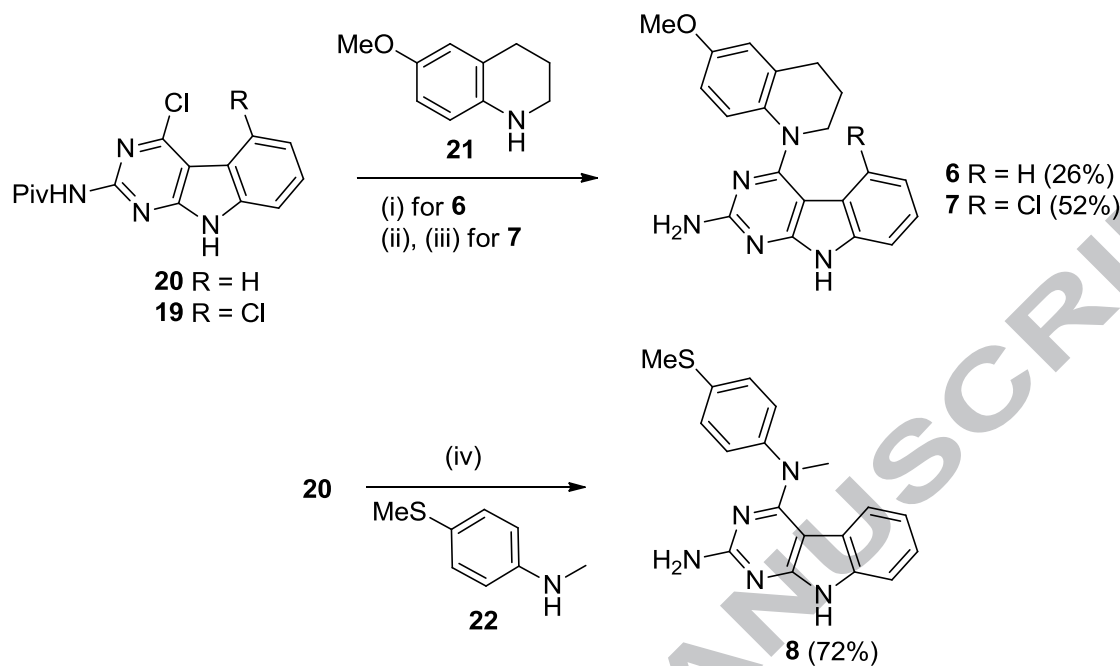
with 4-methoxy-*N*-methyl aniline provided target compounds **2** and **3** in 78% and 38% yields, respectively.

Scheme 2. Synthesis of target compounds **4** and **5**^a



^aReagents and conditions: (i) $\text{CNCH}_2\text{CO}_2\text{Et}$, *t*-BuOK, THF, reflux; (ii) Zn dust, AcOH, 60 °C; (iii) $\text{NH}_2(\text{C}=\text{NH})\text{Cl}\cdot\text{HCl}$, DMSO, 120 °C; (iv) Piv_2O , 120 °C; (v) POCl_3 , reflux; (vi) 4-methoxy-*N*-methylaniline, conc. HCl (2 drops), *i*-PrOH, reflux; (vii) 1 N NaOH, *i*-PrOH, reflux.

The synthesis of target compounds **4** and **5** is shown in Scheme 2. Displacement of the 2-F of commercially available **13** with ethyl cyanoacetate anion provided **14** in 82% yield. Reduction of the nitro group of **14** followed by cyclization furnished the indole **15**. Cyclocondensation of **15** with carbamimidic chloride hydrochloride afforded the 2-amino-4-oxo-pyrido[4,5-*b*]indole **16**. Pivaloyl protection of the 2-NH₂ of **16** gave **17**, which, upon chlorination at the 4-position, provided **18** in 86% yield. Nucleophilic displacement of the 4-Cl of **18** and **19**³³ with 4-methoxy-*N*-methyl aniline provided target compounds **4** and **5**, respectively.

Scheme 3. Synthesis of target compounds **6–8**^a

^aReagents and conditions: (i) compound **21**, conc. HCl (2–3 drops), BuOH, reflux; (ii) compound **21**, conc. HCl (2 drops), *i*-PrOH, reflux; (iii) 1 N NaOH, *i*-PrOH, reflux; (iv) compound **22**, conc. HCl (2 drops), BuOH, reflux.

Displacement of the 4-Cl group of **20**²⁹ (Scheme 3) with 6-methoxy-1,2,3,4-tetrahydroquinoline **21** and concomitant deprotection of the pivaloyl group from the 2-NH₂ group afforded target compound **6** in 26% yield. Treatment of **19** (Scheme 2) with **21**, followed by base-mediated deprotection of the 2-NH₂ group, provided target compound **7** in 52% yield. Compound **8** was obtained by treating **20**²⁹ with 4-thiomethyl-*N*-methylaniline **22**³⁴ in BuOH at reflux.

Effect on cellular microtubules and cancer cell proliferation. Compounds **2–8** were evaluated for their ability to depolymerize microtubules in A-10 smooth muscle cells with a phenotypic assay that measures the percent cellular microtubule loss. An EC₅₀, the concentration

that causes 50% cellular microtubule loss, was determined. The antiproliferative effects in MDA-MB-435 melanoma cells using the sulforhodamine B (SRB) assay and the IC_{50} , the concentration that cause 50% inhibition of proliferation was determined. The activities of the compounds were compared with **1**, paclitaxel and CA-4 (Table 1).

Table 1. Microtubule depolymerizing activities (EC_{50}) and antiproliferative values (IC_{50}) of **2–8**.

Compd	EC_{50} for microtubule depolymerization (nM)	MDA-MB-435 $IC_{50} \pm SD$ (nM)	EC_{50}/IC_{50} Ratio
1 ^a	130	14.7 ± 1.5	8.8
2	130	33.9 ± 3.4	3.8
3	1200	130 ± 7.8	9.2
4	1400	220 ± 25	6.5
5	No effects up to 40 μ M	3,900 ± 200	
6	150	54.4 ± 4	2.8
7	3700	271 ± 4	15
8	1100	89.1 ± 10	12
paclitaxel ^b		4.5 ± 0.5	
CA-4 ^b	9.8	4.4 ± 0.5	2.2

^aResults previously published.²⁹ ^bResults previously published.³⁵

The 2-Me analog **2** has a 2-fold lower potency for cancer cell cytotoxicity than the 2-NH₂ **1**, but was equipotent with **1** for effects on cellular microtubules and had a lower EC_{50}/IC_{50} ratio, 3.8 as compared to 8.8 for **1** and this indicates an improved correlation between the microtubule depolymerizing effects and the cancer cell cytotoxicity. The 2-H analog **3** displayed ~10-fold lower potency in both cell proliferation and microtubule depolymerizing assays, than the 2- NH₂

1, indicating the importance of the size of the substitution at the 2-position for microtubule depolymerizing activity among compounds **1–3**. Replacement of the 5-H of **1** with a 5-Me (**4**) resulted in 15- and 11-fold lower antiproliferative and microtubule depolymerizing potencies, respectively. Substitution of a 5-Cl (**5**) moiety for the 5-H of **1** resulted in a 263-fold loss of potency for the antiproliferative effects and no effects on cellular microtubules at concentration up to 40 μM . These data indicate that substitution of a Me or Cl at the 5-position results in decreased potency, perhaps as a consequence of steric hindrance and/or conformational restriction of the rotation of the bonds (a) and/or (b) (Figure 2). Compound **6**, the tetrahydroquinoline substituted is conformationally restricted around bond (b) and is a 5-unsubstituted analog, that allows rotation of the (a) bond, is only marginally less active than **1** and **2** for microtubule loss and for inhibiting MDA-MB-435 tumor cells (Table 1). Further, conformationally restricted **7**, the 5-Cl substituted analog, was significantly less potent than **1** and **6** against MDA-MB-435 tumor cells and was less potent at inhibiting microtubule loss as well. Compound **6** compared to **7** was markedly more potent indicating that conformational restriction of the N^4 -phenyl moiety about (b) bond with a 1,2,3,4-tetrahydroquinoline group is only slightly detrimental to activity. However, further conformational restriction of (a) bond via 5-position substitution as in **7** significantly decreases activity. These results together with the results obtained with the 5-substituted compounds **4** and **5** suggest that conformational restriction of the (b) bond is not particularly detrimental to MDA-MB-435 antiproliferative activity (compare **6** with **1** and **2**) but further conformational restriction via the (a) bond is detrimental. The 5-position Me and Cl substitution in **4**, **5** and **7** could also cause steric hindrance to binding at the tubulin site which could also contribute to their lower activities. Replacement of the 4'-

OMe of **1** with a 4'-SMe group (**8**) resulted in a 6-fold decrease in activity (IC_{50}), clearly indicating that this isosteric replacement of the OMe with a SMe is not conducive to activity.

Inhibition of tubulin assembly and colchicine binding. On the basis of their microtubule depolymerizing activities, compounds **2**, **3**, **6** and **8** were evaluated for their direct effects on tubulin assembly and inhibition of colchicine binding (Table 2). Compound **2** inhibited tubulin assembly with activity comparable to the lead compound **1** and CA-4. Compounds **3**, **6** and **8** were marginally (1.6-fold) less potent than **1** as inhibitors of tubulin assembly. Compounds **2**, **3**, **6** and **8** inhibited the binding of [3H]colchicine to tubulin by 62–71%, whereas the lead compound **1** showed 84% inhibition of [3H]colchicine binding. These data indicate that the target compounds **2**, **3**, **6** and **8** have somewhat less affinity for the colchicine site as compared to **1**.

Table 2. Inhibition of tubulin assembly and colchicine binding.

Compd	Inhibition of tubulin assembly $IC_{50} \pm SD$ (μM)	Inhibition of colchicine binding (% inhibition $\pm SD$) at 5 μM
1 ^a	1.4 \pm 0.007	84 \pm 0.5
2	1.2 \pm 0.04	67 \pm 5
3	2.3 \pm 0.4	62 \pm 4
6	2.2 \pm 0.1	71 \pm 5
8	2.3 \pm 0.3	67 \pm 5
CA-4 ^a	1.0 \pm 0.09	99 \pm 0.2

^aResults previously published.²⁹ ^bND: not determined.

Effect on Pgp and β III-tubulin mediated drug resistance in cancer cells. Pgp and β III-tubulin-mediated drug resistance were observed clinically with the taxanes and vinca alkaloids.³⁶ MTAs that are not sensitive to these drug resistance mechanisms would be beneficial in tumors resistant to other MTAs because of these mechanisms. Hence, target compounds were evaluated for the ability to overcome Pgp or β III-tubulin-mediated resistance in isogenic SK-OV-3 and HeLa cell line pairs, respectively using the SRB assay (Table 3).³⁷ The relative resistance value, designated Rr, was calculated by dividing the IC₅₀ obtained in the Pgp-expressing SK-OV-3 MDR-1-M6/6 cells by the IC₅₀ obtained in the parental SK-OV-3 ovarian cancer cells. In the SK-OV-3 cell line pair, the Pgp-expressing cells are resistant to paclitaxel, with a Rr value of 240, demonstrating the high susceptibility of paclitaxel to Pgp-mediated transport. Target compounds **2**, **3**, **6** and **8** had Rr values of less than 2, similar to that observed with CA-4.

Table 3. Target compounds **2**, **3**, **6** and **8** circumvent Pgp and β III-tubulin mediated resistance.

Compd	IC ₅₀ ± SD (nM)		Rr	IC ₅₀ ± SD (nM)		
	SK-OV-3	SK-OV-3-MDR1-M6/6		HeLa	HeLa WT β III	Rr
1 ^a	27.6 ± 1.8	34.4 ± 5.9	1.2	21.3 ± 2.2	21.4 ± 3.5	1.0
2	60.5 ± 2.4	78.0 ± 8.4	1.3	50.5 ± 5.3	31.8 ± 2.5	0.6
3	173 ± 8.6	224 ± 21	1.4	142 ± 8.1	99.5 ± 12	0.8
6	83.2 ± 5.7	135 ± 23	1.6	72.1 ± 7.9	87.0 ± 4.1	1.2
8	156 ± 16	160 ± 15	1	118 ± 13	78.4 ± 4	0.7
paclitaxel ^b	5.0 ± 0.6	1,200 ± 58	240	2.8 ± 0.4	24.0 ± 3	8.6
CA-4 ^b	5.5 ± 0.5	7.2 ± 1.1	1.3	3.3 ± 0.4	3.3 ± 0.3	1

^aResults previously published.²⁹ ^bResults previously published.³⁵

A HeLa cell line pair was used to evaluate the effects of β III-tubulin on the sensitivity of the cell line for **2**, **3**, **6** and **8** (Table 3). The IC_{50} of each of these compounds were determined and the relative resistance (R_r) value was calculated by dividing the IC_{50} of the β III-tubulin expressing cells by the IC_{50} value obtained in HeLa parental cells. Paclitaxel is less potent in the β III-tubulin expressing cells with a R_r value of 8.6. On the other hand, compounds **2**, **3**, **6** and **8** had R_r values of ≈ 1.0 implying equal sensitivity to the β III-tubulin expressing cell line. These data suggest that these compounds overcome both Pgp and β III-tubulin mediated resistance and in that regard, have advantages over the paclitaxel.

To rationalize the structure-activity relationships summarized above, docking of target compounds **2–8** was carried out in the X-ray crystal structure of colchicine in the colchicine site of tubulin (PDB: 4O2B,³⁸ 2.30 Å) using Molecular Operating Environment (MOE 2015.10).³⁹ Multiple low energy conformations were obtained on docking. The protein was prepared as reported previously.³⁵ Ligands were sketched using the builder function in MOE and minimized using the Amber10:EHT forcefield. The ligands were then docked in the binding site using the default settings in the docking protocol. The placement was performed using Triangle Matcher and scored using London dG. The refinement was carried out using Rigid Receptor and scored using GBVI/WSA dG. To validate the docking study at the colchicine site, the native ligand colchicine was re-docked into the binding site using the same set of parameters as described above. The rmsd of the best docked pose was 0.345 Å, thus validating docking using MOE.

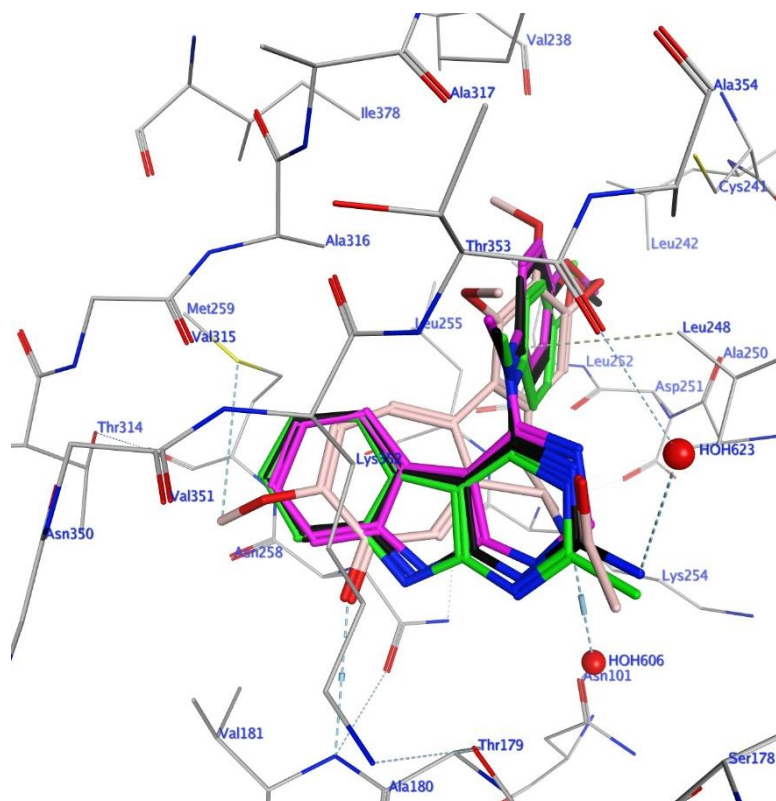


Figure 3. Superimposition of the docked poses of **1** (black), **2** (green) and **3** (magenta) in the colchicine (pink) binding site of tubulin (PDB ID: 4O2B).

Figure 3 shows the superimposed docked poses of **1** (black), **2** (green) and **3** (magenta) in the colchicine site of tubulin (PDB: 4O2B,³⁸ 2.30 Å). The pyrimido[4,5-*b*]indole scaffold of **1**, **2** and **3** forms hydrophobic interactions with Ala α 180, Val α 181, Leu β 248, Asn β 258, Met β 259, Thr β 314 and Lys β 352 and overlaps with the C-ring of colchicine. The *N*⁴-Me group lies in a pocket lined by hydrophobic residues Leu β 248 and Ala β 354. The *N*⁴-aryl moiety makes hydrophobic interactions with Cys β 241, Ala β 250, Leu β 255, and Ala β 316 and overlaps with ring A of colchicine. The 4'-OMe group points towards residues Cys β 241, Leu β 242 and Leu β 255 and superposes with the 3-OMe group of colchicine. The 2-NH₂ of **1** undergoes hydrogen bonding with HOH623. The 2-Me group in **2** retains hydrophobic interactions with Leu β 248 (3.90 Å) and Ser α 178 (3.99 Å). For compound **3**, the 2-H group is incapable of hydrogen bonding or hydrophobic interactions with the surrounding residues, and this results in a 10-fold loss in both

the IC_{50} and EC_{50} compared to **1** with its 2-NH₂ moiety. The best docked poses of **1**, **2** and **3** had scores of -7.08 kcal/mol, -7.18 kcal/mol and -6.84 kcal/mol, respectively, which suggests lower affinity of **3** and similar affinity of **1** and **2** in the colchicine site.

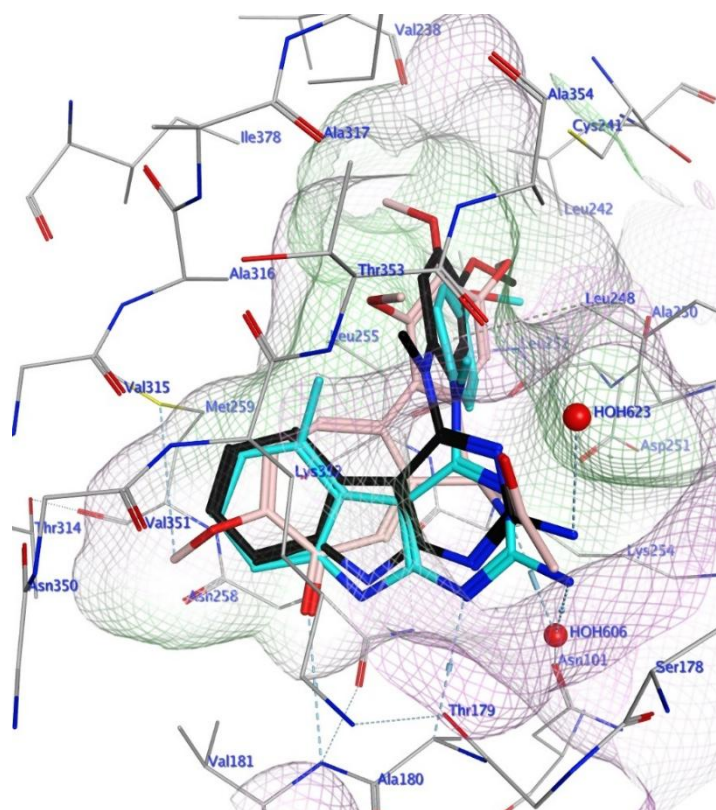


Figure 4. Superimposition of the docked poses of **1** (black) and **4** (cyan) in the colchicine (pink) site of tubulin (PDB ID: 4O2B). Hydrophobic surface is in green and hydrophilic surface is in pink.

Figure 4 shows the superimposed docked poses of **1** (black) and **4** (cyan) in the colchicine site of tubulin. Compound **4** retains the key binding interactions at the colchicine site as described for **1** in Figure 3. The 2-NH₂ of **1** undergoes hydrogen bonding with HOH623, whereas the 2-NH₂ of **4** undergoes hydrogen bonding with HOH606. The lower activity of **4** and **5** as compared to **1** can be rationalized in part, on the basis of a small hydrophobic pocket in the binding site. The 5-Me in **4** lies in a hydrophobic pocket lined by residues Met β 259, Ala β 316

and Lys β 352. This small hydrophobic pocket results in steric hindrance probably leading to high energy conformations for **4** and **5**, resulting in lower activities of **4** and **5** as compared to **1**. In addition, the best docked pose of **4** had a score of -5.96 kcal/mol which is higher (worse) than the score (-7.08 kcal/mol) for the best docked pose of **1**.

Structural explanation of activity with conformational preferences from ^1H NMR data.

The ^1H NMR spectra of the target compounds **2–8**, the lead N^4 -Me compound **1** and the N^4 -H compound **23** (Figure 5) in $\text{DMSO-}d_6$ provided valuable information regarding the role of conformational restriction in microtubule depolymerization activity of the tricyclic pyrimido[4,5-*b*]indoles. The N^4 -Me compound **1** showed excellent microtubule depolymerization and tumor cell inhibitory activities compared to the N^4 -H analog **23**.²⁹ This difference could be attributed, in part, to conformational restriction of the bonds connecting the nitrogen to the pyrimidine ring (a) (N-C4) and to the phenyl ring (b) (N-C1') (Figure 5). The (a) and (b) bonds in **1** are somewhat restricted compared to those in **23** due to the presence of steric bulk of the N^4 -Me group. For **23**, the “5-H” proton appears at $\delta > 6.80$, whereas for **1**, it is more shielded at $\delta = 5.75$. This shielding of the “5-H” proton in **1** is due to the diamagnetic anisotropy in **1** arising from the orientation of the phenyl ring as depicted by the more favored conformation of **1** in Figure 5. The steric bulk of the N^4 -Me in **1** restricts the conformation and thus positions the phenyl group on top of the 5-H moiety, resulting in the observed shielding effect on the 5-H group.

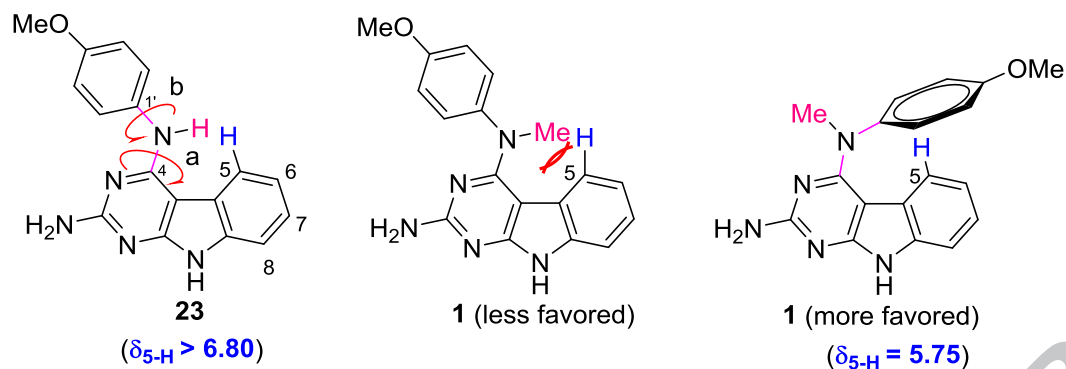


Figure 5. Conformational restriction of C4-N (a) and N-C1' (b) bonds in the presence of the N^4 -Me moiety and δ values (^1H NMR) of the 5-H group for **1** and **23**.

For target compounds **2** (2-Me) and **3** (2-H), conformational restriction of bond (a) due to the N^4 -Me causes shielding of the “5-H” proton ($\delta = 5.90$, ^1H NMR, Figure 6) similar to that observed in **1**.

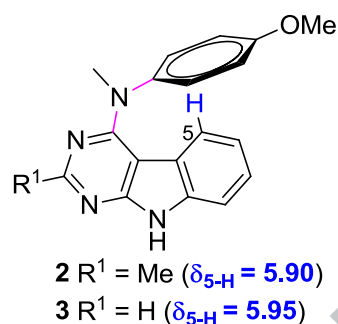


Figure 6. Shielding (δ values, ^1H NMR) of the 5-H proton in **2** and **3**.

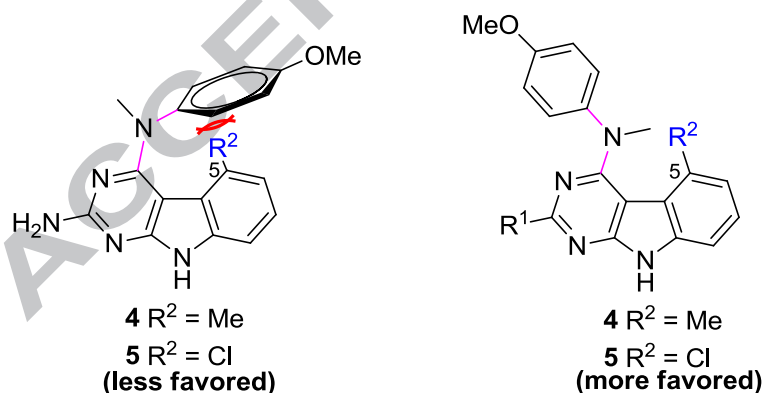


Figure 7. Substitution at the 5-position hinders the free rotation of the N^4 -aryl moiety.

Compounds **4** and **5** were less active than **1** due to increased hydrophobicity and/or steric hindrance caused by the 5-Me and 5-Cl groups, respectively. The steric hindrance resulting from the 5-Me (**4**) or the 5-Cl (**5**) group conformationally restricts rotation around bond (b) and decreases the total number of low energy conformations for **4** and **5** (Figure 7). Conformational search of **1**, **4** and **5** was carried out using Sybyl-X 2.1.1⁴⁰ (default protocol) to assess the number of low energy conformations within 1 kcal/mol or 5 kcal/mol with 1° rotation about (a) bond (Table 4). Compounds **4** and **5** both had a lower number of conformations than **1** due to the steric hindrance, thus making the adoption of the bioactive conformation(s) for **4** and **5** in the colchicine site more difficult thus contributing to the lower affinity compared to **1**. Clearly the 5-Me and 5-Cl moieties may also cause steric hindrance to tubulin binding which could also contribute to the lower activities of **4** and **5** compared to **1**. The lower potency of the 4'-SMe analog **8** is attributed to the isosteric replacement of the 4'-OMe in **1** as discussed above, since, the conformational profile of **8** (calculated using Sybyl-X 2.1.1) was similar to that of **1**.

Table 4. Systematic Search (conformations) allowing 1 degree rotation of C₄-N- C₁' (of pyrimido indole moiety) using Sybyl-X 2.1.1.

Compd	Conformations within	Conformations within
	1 kcal/ mol	5 kcal/ mol
1 (5-H)	31	65
4 (5-Me)	22	37
5 (5-Cl)	15	43

In conclusion, we reported the design, synthesis and structure–activity relationship (SAR) of substituted tricyclic pyrimido[4,5-*b*]indoles as microtubule depolymerizers. Compound **2**, containing the 2-Me group, was as potent as the 2-NH₂ analog **1** and both **1** and **2** were better than the 2-H analog **3**, which indicates that substitution at the 2-position with a 2-Me or 2-NH₂ is important for activity. Substitution at the 5-position of the pyrimido[4,5-*b*]indole scaffold with a 5-Me or 5-Cl is detrimental for activity. Conformational restriction of the *N*⁴-aryl group using a 1,2,3,4-tetrahydroquinoline moiety without a 5-substitution (**6**) only marginally decreased potency compared to **1** and **2** in the MDA-MB-435 tumor cell lines. Compound **7** with similar bond restriction as **6**, but with a sterically bulky 5-Cl substitution substantially decreased activity. Replacement of the 4'-OMe with a 4'-SMe group (**8**) also resulted in an increased EC₅₀ for microtubule depolymerization, indicating the probable role of hydrogen bonding of the 4'-OMe and/or large size interaction with tubulin at this position. Proton NMR and molecular modeling were utilized to explain how subtle structural changes of the substituents on the pyrimido[4,5-*b*]indole scaffold affected the microtubule depolymerization and MDA-MB-435 inhibitory activity. This SAR information will be employed to design the next series of tricyclic pyrimido[4,5-*b*]indoles with improved microtubule depolymerizing and tumor cell inhibitory activities.

Acknowledgements. This work was supported, in part, by a grant from the National Institutes of Health, National Cancer Institute (CA142868 (AG, SLM)); by the Duquesne University Adrian Van Kaam Chair in Scholarly Excellence (AG); and by an NSF equipment grant for NMR instrumentation (NMR: CHE 0614785).

Disclaimer. The content of this paper is solely the responsibility of the authors and does not necessarily reflect the official views of the National Institutes of Health.

References

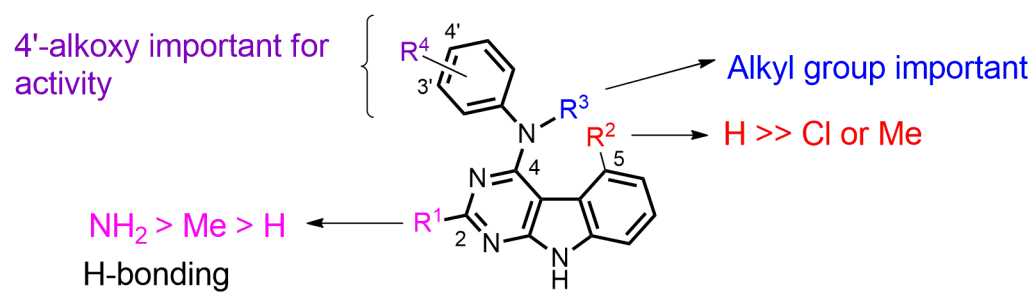
1. Dumontet, C.; Jordan, M. A. *Nat. Rev. Drug Discov.* **2010**, *9*, 790-803.
2. Field, J. J.; Kanakkanthara, A.; Miller, J. H. *Bioorg. Med. Chem.* **2014**, *22*, 5050-5059.
3. Bowne-Anderson, H.; Hibbel, A.; Howard, J. *Trends Cell Biol.* **2015**, *25*, 769-779.
4. Komlodi-Pasztor, E.; Sackett, D.; Wilkerson, J.; Fojo, T. *Nat. Rev. Clin. Oncol.* **2011**, *8*, 244-250.
5. Wang, Z.; Sun, Y. *Transl. Oncol.* **2010**, *3*, 1-12.
6. O'Connor, P. M.; Jackman, J.; Bae, I.; Myers, T. G.; Fan, S.; Mutoh, M.; Scudiero, D. A.; Monks, A.; Sausville, E. A.; Weinstein, J. N.; Friend, S.; Fornace, A. J.; Kohn, K. W. *Cancer Res.* **1997**, *57*, 4285-4300.
7. Lee, J. F. and Harris, L. N. Antimicrotubule agents. In *Cancer: Principles & Practice of Oncology* 8th Ed., V. T. DeVita, Jr., T. S. Lawrence and S. A. Rosenberg Eds., Lippincott Williams & Wilkins, **2008**, 447-456.
8. Dybdal-Hargreaves, N. F.; Risinger, A. L.; Mooberry, S. L. *Clin. Cancer Res.* **2015**, *21*, 2445-2452.
9. Doodhi, H.; Prota, A. E.; Rodriguez-Garcia, R.; Xiao, H.; Custar, D. W.; Bargsten, K.; Katrukha, E. A.; Hilbert, M.; Hua, S.; Jiang, K.; Grigoriev, I.; Yang, C. P.; Cox, D.; Horwitz, S. B.; Kapitein, L. C.; Akhmanova, A.; Steinmetz, M. O. *Curr. Biol.* **2016**, *26*, 1713-1721.

10. Prota, A. E.; Bargsten, K.; Diaz, J. F.; Marsh, M.; Cuevas, C.; Liniger, M.; Neuhaus, C.; Andreu, J. M.; Altmann, K.-H.; Steinmetz, M. O. *Proc. Natl. Acad. Sci.* **2014**, *111*, 13817-13821.
11. Verma, S.; Miles, D.; Gianni, L.; Krop, I. E.; Welslau, M.; Baselga, J.; Pegram, M.; Oh, D.-Y.; Diéras, V.; Guardino, E.; Fang, L.; Lu, M. W.; Olsen, S.; Blackwell, K. *N. Engl. J. Med.* **2012**, *367*, 1783-1791.
12. Cortes, J.; O'Shaughnessy, J.; Loesch, D.; Blum, J. L.; Vahdat, L. T.; Petrakova, K.; Chollet, P.; Manikas, A.; Diéras, V.; Delozier, T.; Vladimirov, V.; Cardoso, F.; Koh, H.; Bougnoux, P.; Dutcus, C. E.; Seegobin, S.; Mir, D.; Meneses, N.; Wanders, J.; Twelves, C. *Lancet* **2011**, *377*, 914-923.
13. Thomas, C.; Movva, S. *Onco Targets Ther.* **2016**, *9*, 5619-5627.
14. Lu, Y.; Chen, J.; Xiao, M.; Li, W.; Miller, D. *Pharm. Res.* **2012**, *29*, 2943-2971.
15. Massarotti, A.; Coluccia, A.; Silvestri, R.; Sorba, G.; Brancale, A. *ChemMedChem* **2012**, *7*, 33-42.
16. Liu, P. Q., Y.; Wu, L.; Yang, S.; Li, N.; Wang, H.; Xu, H.; Sun, K.; Zhang, S.; Han, X.; Sun, Y.; Shi, Y. *Anticancer Drugs* **2014**, *25*, 462-471.
17. Ng, Q.-S.; Mandeville, H.; Goh, V.; Alonzi, R.; Milner, J.; Carnell, D.; Meer, K.; Padhani, A. R.; Saunders, M. I.; Hoskin, P. J. *Ann. Oncol.* **2012**, *23*, 231-237.
18. Nathan, P.; Zweifel, M.; Padhani, A. R.; Koh, D.-M.; Ng, M.; Collins, D. J.; Harris, A.; Carden, C.; Smythe, J.; Fisher, N.; Taylor, N. J.; Stirling, J. J.; Lu, S.-P.; Leach, M. O.; Rustin, G. J. S.; Judson, I. *Clin. Cancer Res.* **2012**, *18*, 3428-3439.

19. Zweifel, M.; Jayson, G. C.; Reed, N. S.; Osborne, R.; Hassan, B.; Ledermann, J.; Shreeves, G.; Poupard, L.; Lu, S.-P.; Balkissoon, J.; Chaplin, D. J.; Rustin, G. J. S. *Ann. Oncol.* **2011**, *22*, 2036-2041.
20. Patterson, D. M.; Zweifel, M.; Middleton, M. R.; Price, P. M.; Folkes, L. K.; Stratford, M. R. L.; Ross, P.; Halford, S.; Peters, J.; Balkissoon, J.; Chaplin, D. J.; Padhani, A. R.; Rustin, G. J. S. *Clin. Cancer Res.* **2012**, *18*, 1415-1425.
21. Bruce, J.; Eickhoff, J.; Pili, R.; Logan, T.; Carducci, M.; Arnott, J.; Treston, A.; Wilding, G.; Liu, G. *Invest. New Drugs* **2012**, *30*, 794-802.
22. Harrison, M.; Hahn, N.; Pili, R.; Oh, W.; Hammers, H.; Sweeney, C.; Kim, K.; Perlman, S.; Arnott, J.; Sidor, C.; Wilding, G.; Liu, G. *Invest. New Drugs* **2011**, *29*, 1465-1474.
23. Rohena, C. C.; Mooberry, S. L. *Nat. Prod. Rep.* **2014**, *31*, 335-355.
24. Zhao, Y.; Mu, X.; Du, G. *Pharmacol. Ther.* **2016**, *162*, 134-143.
25. Patel, N. H.; Rothenberg, M. L. *Invest. New Drugs* **1994**, *12*, 1-13.
26. Kavallaris, M. *Nat. Rev. Cancer* **2010**, *10*, 194-204.
27. Fojo, T.; Menefee, M. *Ann. Oncol.* **2007**, *18*, 3-8.
28. Stengel, C.; Newman, S. P.; Leese, M. P.; Potter, B. V. L.; Reed, M. J.; Purohit, A. *Brit. J. Cancer* **2010**, *102*, 316-324.
29. Gangjee, A.; Zaware, N.; Devambatla, R. K. V.; Raghavan, S.; Westbrook, C. D.; Dybdal-Hargreaves, N. F.; Hamel, E.; Mooberry, S. L. *Bioorg. Med. Chem.* **2013**, *21*, 891-902.
30. Gangjee, A.; Zhao, Y.; Raghavan, S.; Rohena, C. C.; Mooberry, S. L.; Hamel, E. *J. Med. Chem.* **2013**, *56*, 6829-6844.
31. Showalter, H. D. H.; Bridges, A. J.; Zhou, H.; Sercel, A. D.; McMichael, A.; Fry, D. W. *J. Med. Chem.* **1999**, *42*, 5464-5474.

32. Tichý, M.; Pohl, R.; Xu, H. Y.; Chen, Y.-L.; Yokokawa, F.; Shi, P.-Y.; Hocek, M. *Bioorg. Med. Chem.* **2012**, *20*, 6123-6133.
33. Gangjee, A.; Zaware, N.; Raghavan, S.; Ihnat, M.; Shenoy, S.; Kisliuk, R. L. *J. Med. Chem.* **2010**, *53*, 1563-1578.
34. Abdel-Magid, A. F.; Carson, K. G.; Harris, B. D.; Maryanoff, C. A.; Shah, R. D. *J. Org. Chem.* **1996**, *61*, 3849-3862.
35. Devambatla, R. K. V.; Namjoshi, O. A.; Choudhary, S.; Hamel, E.; Shaffer, C. V.; Rohena, C. C.; Mooberry, S. L.; Gangjee, A. *J. Med. Chem.* **2016**, *59*, 5752-5765.
36. Perez, E. A. *Mol. Cancer Ther.* **2009**, *8*, 2086-2095.
37. Risinger, A. L.; Jackson, E. M.; Polin, L. A.; Helms, G. L.; LeBoeuf, D. A.; Joe, P. A.; Hopper-Borge, E.; Luduena, R. F.; Kruh, G. D.; Mooberry, S. L. *Cancer Res.* **2008**, *68*, 8881-8888.
38. Prota, A. E.; Danel, F.; Bachmann, F.; Bargsten, K.; Buey, R. M.; Pohlmann, J.; Reinelt, S.; Lane, H.; Steinmetz, M. O. *J. Mol. Biol.* **2014**, *426*, 1848-1860.
39. Molecular Operating Environment (MOE 2013.08); Chemical Computing Group, Inc.: Montreal, Quebec, Canada, 2013; www.chemcomp.com.
40. SYBYL-X 2.1.1, Tripos International, 1699 South Hanley Rd., St. Louis, Missouri, 63144, USA.

Supplementary Material. Experimental procedures for the synthesis, compound characterization, and biological evaluation of the target compounds. This material is available free of charge via the Internet.



ACCEPTED MANUSCRIPT